

Phenol Removal from liquid waste of Petrochemical company using Hydrophobic PVDF Membrane Incorporated with TiO₂ and FTPs via VMD

Elham El-Zanati , Maaly Khedr ,Eman Farag and Esraa Taha

Department of Chemical Engineering and Pilot Plant, Engineering Research Division, National Research Centre, Dokki, Giza, Egypt.

Received: 5 April. 2023, Revised: 18 May. 2023, Accepted: 21 Jun. 2023.

Published online: 1 Jul. 2023.

Abstract: Because low pressure and temperature were necessary, membrane distillation (MD) was used to concentrate phenolic-rich solution. The fabricated PVDF/TiO₂ membranes with and without silane modification were evaluated for their separation abilities. Prior to blending into the PVDF casting solution, the TiO₂ nanoparticles were either used as it is or hydrophobic modified. the PVDF/TiO₂ membrane with silane modification had a water contact angle of (118°C), whereas the membrane incorporated with hydrophobic modified TiO₂ (PVDF/FTP) had nearly super hydrophobicity (122°C).

Using a phenolic-rich solution, the separation performance of these membranes was evaluated in MD. Significant phenolic compounds rejection was shown by all membranes, ranging from 65% to 99%. In comparison to the unmodified PVDF/TiO₂ membrane, the modified PVDF/TiO₂ with silane solution and PVDF/FTP membranes displayed flux (8.9 and 10.5 lit/m².h, respectively). The maximum permeation flux, however, was attained by the PVDF/ FTP membrane because it formed a large amount of porosity during phase inversion without being disturbed by silane alteration.

Keywords: Petrochemical, FTPs, VMD.

1 Introduction

The World Health Organization has advised that 1 µg/L is the maximum allowable concentration of phenolics in drinking water [1], and the Environmental Protection Agency's requirements require phenolic contents in wastewater to be reduced to less than 1 mg/L [2]. To safeguard the environment and public health, it is crucial to remove phenols from water and wastewater. For the elimination of phenol, numerous treatment techniques have been used. Activated carbon adsorption [3], chemical oxidation [4], membrane process [5], and biological treatment [4] are popular methods among these.

The approaches mentioned above are accompanied by issues such high cost, poor efficiency, and harmful byproduct formation [6]. For wastewater from petrochemical, pharmaceutical, and refinery operations, which often has a high phenol concentration, biological treatment is typically not appropriate [7]. Chemical oxidation needs a lot of oxidizing chemicals and operates at high temperatures [8], and there's a chance that incomplete oxidation could lead to more harmful byproducts. Meanwhile, activated carbon adsorption can efficiently remove organic chemicals like phenol, but this approach has a disadvantage in that it is expensive and challenging to regenerate due to phenol chemisorption and the breakdown of carbon [9].

For the treatment of phenolic wastewater, membrane separation techniques such as reverse osmosis, ultrafiltration, and pervaporation have gained increased attention [10]. Membrane distillation (MD) was also applied to concentrate phenolic rich solution because of the requirement of low pressure and temperature. Vacuum membrane distillation (VMD) is a membrane process that uses microporous hydrophobic membranes to extract volatile

Corresponding author-mail:

chemicals and water vapour from aqueous solutions. Because the membrane is hydrophobic, liquid cannot enter the pores.

When a partial pressure differential is generated across a membrane by providing vacuum on the opposite side, both water vapour and volatile species begin to permeate through the membrane pores (see Figure 1). Because of the exponential relationship between vapour pressure and temperature, vapour mass diffusion (VMD) is not constrained by the osmotic pressure of the feed. The following are the key benefits of MD over traditional separation methods [4]:

- Complete separation of cells, macromolecules, colloids, ions, etc. To put it another way, it yields distillate of high quality.
- At relatively low temperatures, water can be distilled.
- It is possible to employ low-grade heat, such as solar, industrial waste heat, or desalination waste heat. As opposed to pressure-based membrane treatment procedures, the water does not need considerable preparation.

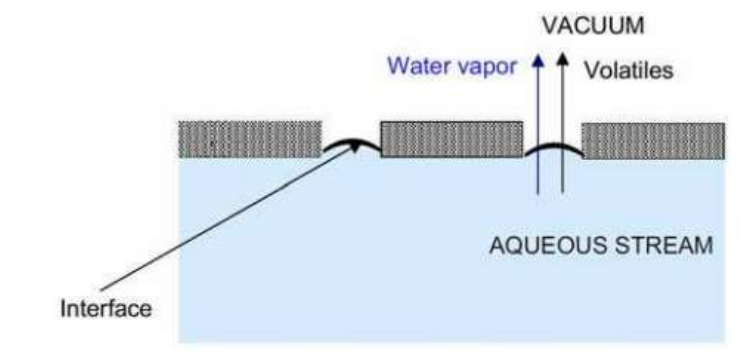


Fig.1: Permeation of water vapor and volatile species by VMD [28].

Due to its high operability and tunable membrane forming qualities, polyvinylidene fluoride (PVDF) is used extensively in VMD. In an effort to modify the membrane structure and enhance its qualities, appropriate additives are added to the PVDF dope solution as part of efforts to improve the mechanical properties of PVDF membranes. To strengthen the structure of PVDF membranes, mixed matrix membranes including nanoparticles were created. The insertion of metal oxide particles to improve membrane function is one of the most flexible and successful modification procedures. PVDF has been combined with aluminum oxide (Al_2O_3), zirconium dioxide (ZrO_2), and titanium dioxide (TiO_2) to create membranes with improved performance, mechanical stability, and thermal characteristics.

In this research, different PVDF/ TiO_2 composite membranes were evaluated in VMD separation process for treatment of phenolic wastewater. The effects of membrane type, feed temperature and feed phase pH were also studied.

2 Materials and Methods:

2.1 Materials

PVDF powder (Solef, PVDF) was supplied by Alfa Aesar. N-methyl-2-pyrrolidone (NMP) (>99.5%), ortho-Phosphoric acid (H_3PO_4) (>85%), ethanol (>99.9%), acetone was purchased from Merck (Darmstadt, Germany). TiO_2 nanoparticles (<150 nm particle size, >99.5% trace metal basis) were acquired from Sigma-Aldrich. Silane solution (heptadecafluoro-1,1,2,2-tetrahydrodecyl) triethoxysilane (FAS) from Sigma-Aldrich. Phenol detached crystals, extra pure 99.5%, purchased from Loba Chemie, INDIA.

2.2 Hydrophobic modification for TiO_2 nanoparticles preparation:

The hydrophobic modified TiO_2 particles by FAS (FTPs) were created by adding 40 g of TiO_2 particles to a silane solution of 100 ml of ethanol that contained 1 ml of FAS. The solution mixture was aggressively agitated at 50°C for 2 hours at 600 rpm before being repeatedly washed with ethanol and dried at 120°C for 2 hours to produce the

FTPs. These TiO₂ particles are known as FTPs because FAS molecules have partially replaced the hydroxyl groups on the particle surface [11].

2.3 Membranes preparation:

PVDF powder was dried at 100 °C for 6 h to remove its moisture content. The dried PVDF powder was mixed with solvent and non-solvent additive mixture according to Table 1. TiO₂ loading was added at 3% as the widely used percent in literature ranged from 2-4%. The dope solution was stirred continuously for 8 h at 55 °C and degassed for 24 h. The degassed dope solution was cast on a glass plate of 400 μm at room temperature. The cast film was immersed into coagulation bath of distilled water for 24 h. The precipitated membrane was removed from the coagulation bath and rinsed with distilled water to remove the residual solvent and non-solvent additives. The wet membrane then was dried in the air for one day.

For first modification to prepare P₂ membrane, the PVDF membrane blended with unmodified TiO₂ (P2) produced was immersed in the silane solution (100 ethanol: 1 ml FAS) for (10, 15, 30) min. The membrane was rinsed with ethanol and dried in the oven at 80° C for 2 hrs. before being used.

For sconded modification to prepare P₃ membrane, the fluorinated TiO₂ particles (FTPs) were used as a filler instead of commercial TiO₂ nanoparticles to prepared P3 membranes.

Table 1: compositions of dope solution

Membrane ID	PVDF	NMP	Acetone	H ₃ PO ₄	TiO ₂
P ₁	15	74	5	3	3 (un modified TiO ₂)
P ₂ (silane treatment)	15	74	5	3	3 (un modified TiO ₂)
P ₃	15	74	5	3	3 (flourinated TiO ₂)

3 Membrane Characterizations:

3.1 FTIR

The phases of the virgin and treated TiO₂ particles were investigated using a Fourier-transform infrared (FT-IR) spectroscope (Burker vertex 70). Each spectrum was obtained in transfer mode by pressing the sample with KBr on a pellet, with signal averaging 4000-400 cm⁻¹ scans at a resolution of 4 cm⁻¹. Transparent films were created using infrared (IR) cards [12].

3.2 Particle size distribution (PSD)

The average diameter and the size distribution of samples were measured by using a particle size analyzer (Nano-ZS, Malvern Instruments Ltd., UK). For measuring Size distribution and zeta potential, the sample was sonicated for 10-20 min. just before assessment [13].

Scanning electronic microscopy (SEM)

The surface topography and membrane morphology were characterized using SEM. To add electrical conductivity, a gold sputtering was applied to the dry samples. Images were captured using a JEOL 5410 SEM operating at 10 kV [14].

3.3 Atomic force microscope (AFM)

Using the AFM, Flexaxiom Nanosurf, and C3000 in dynamic mode (non-contact), the topography of the produced membranes was observed in order to confirm hydrophobic alteration and identify changes to the membrane surface. By using an NCLR rectangular-shaped silicon cantilever with a resonance frequency of 9 kHz, AFM experiments were carried out at room temperature.

3.4 Contact angle (CA)

The contact angles of the prepared PVDF membranes were determined by (SCA 20, OCA 15EC) using the sessile drop method in the preparation and finishing of cellulosic fibers, Textile research Division, NRC. The

volume and contact time were 10 μ L and 10s respectively and this was carried out five times for each measured membrane [12].

3.5 Porosity

The gravimetric method was used to calculate the porosity of the Membrane. The volume of the membrane holes is divided by the total volume of the membrane. Ethanol was used to completely moisten the membranes [15]. After the leftover ethanol on the surface was evaporated, the weight (w_1 , g) of the wetted membrane was measured. After being left in the open air for 15 minutes, the membrane samples were dried and weighed (w_2 , g). Equation (1) could be used to calculate the porosity of electro spun membranes [16].

$$\varepsilon_m = \frac{(w_1 - w_2) / \rho_e}{\frac{w_1 - w_2}{\rho_e} + w_2 / \rho_p} \quad (1)$$

Where:

ρ_p : The density of the PVDF (g/m³)

ρ_e : The density of the ethanol (g/m³)

3.6 Mechanical properties

The tensile properties in terms of tensile stress and tensile strain at break for biofilms were determined using an Instron 34SC-5 universal tensile testing machine, UK, equipped with a load cell of 5 kN and a crosshead speed of 10 mm.min⁻¹, according to ASTM D 882-18. The dumbbell specimens were die-cut from the casted films. Prior to testing, all specimens were conditioned at a temperature of 23 \pm 2°C and 50 \pm 5% relative humidity for at least 24 h. The average of three parallel trails for each film was recorded [17].

4VMD Experiments

The VMD experimental setup is shown in Figure 2. The setup consists of a feed solution that is preheated by heater (MSH-20D, DAIHAN Scientific co, Korea) to maintain constant feed temperature. This is introduced into the membrane through a peristaltic pump with a 14.9 cm³/s flow rate (YT600-1JKZ35, longer pump co, China). A flat sheet membrane module with a 103.8 cm² effective membrane area was used. The rejected flow was recycled to the feed flask. The permeated water vapor was condensed in a condenser (designed and manufactured at the workshop of the National Research Centre, Egypt), which is connected to a low temperature chiller unit (Polyscience LS5, Cole-Parmer, USA). The system was maintained under vacuum using a pump (vacuum pump-SH-V40, SH SCIENTIFIC, Korea) with a pressure of about 1 bar (absolute pressure 0 bar) and connected to the permeate side of the membrane. To study the effect of feeding temperature on the prepared membranes performance, the VMD experiments were conducted at different temperatures of feed (40, 60, 70 and 80°C). Also, regarding to enhance the phenol rejection, an VMD experiment was conducted for feed solution with a PH value of 12.

The permeate volume and absorbance were measured. The water permeation flux (J) was determined using the equation below (1):

$$J = \frac{M}{A \times t} \quad (1)$$

Where J is the permeate flux, lit/(m²·hr), M is the volume of distilled water, lit, A is the membrane area, m², and the time, h.

Concentration was calculated from absorbance -concentration calibration curve which was made by an UV spectrophotometer (6850 UV/Vis spectrophotometer, JENWAY). The phenol removal percent (R) was obtained using the following expression Eq. (2), where C_p ; the final concentration of the permeate stream and C_f ; the initial concentration of the feed. The rejection (R) was determined using the equation below (2):

$$R = \frac{C_f - C_p}{C_f} \times 100 \% \quad (2)$$

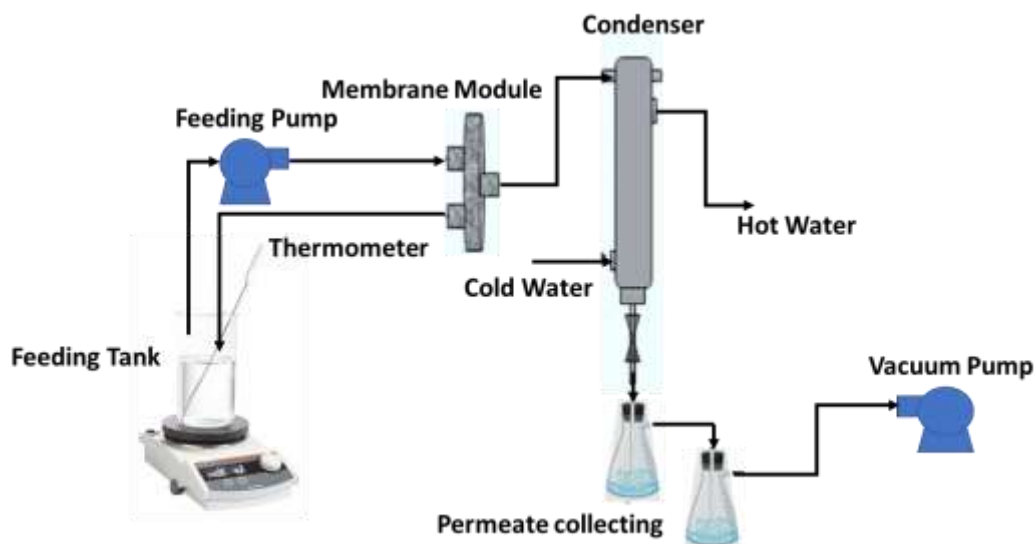


Fig. 2: Schematic diagram for the vacuum membrane distillation system.

5 Result and Discussion

5.1 Fourier transform infrared spectrophotometer (FTIR) of prepared fluorinated TiO_2

The optimal material for MD membranes must have low free surface energy in order to guarantee that the membrane won't become wet during VMD operation. PVDF has a surface energy of 30.3 mN/m, which is higher than polytetrafluoroethylene (PTFE) and polyethylene (PE) [18]. However, PTFE is challenging to manufacture, and polyethylene has a low melting point. PVDF is more easily processed since it can be dissolved in ordinary organic solvents, making it possible to fabricate membranes via a non-solvent induced phase inversion process. To lower the surface energy, self-synthesized Fluorinated TiO_2 nano particles (FTPs) were incorporated into the membrane structure. Fig. 3 and Fig. 4 show the FTIR spectra of the unmodified TiO_2 and Fluorinated TiO_2 nano particles as a hydrophobic enhancer. As illustrated in Figure 4, the band at 950.17 cm^{-1} is attributable to the asymmetric stretching vibration of the Si-O-Ti species, demonstrating the dehydration interaction between FAS molecules and titanium dioxide particles [19,20].

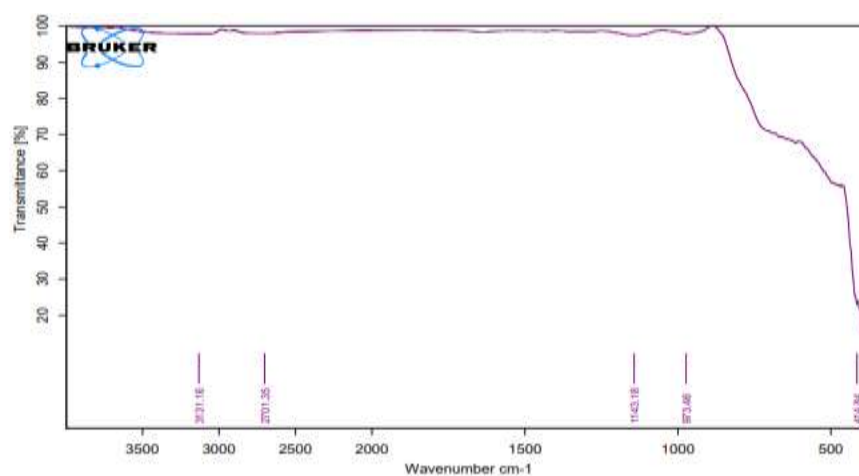


Fig. 3: FTIR spectra of TiO_2 particles.

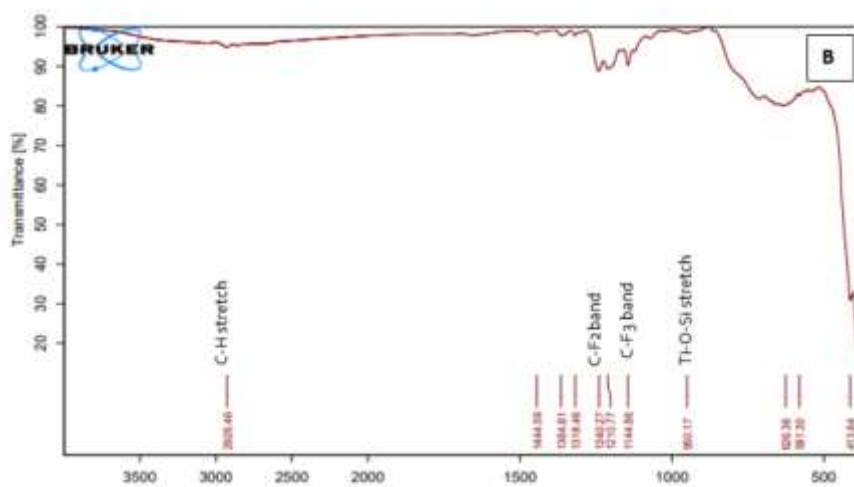


Fig. 4: FTIR spectra of FTNPs particles.

5.2 Particle Size Distribution for FTPs

Dynamic light scattering (DLS) measurements were used to study the TiO₂ nanoparticle size distribution. Figure 5 shows a dynamic light scattering histogram of virgin and modified TiO₂ nanoparticles. As shown in Figure 5. (A), approximately 70.4% of TiO₂ particles were dispersed in the range 50 to 100 nm and had an average particle (hydrodynamic diameter) size of 77.15 nm with a Polydispersity Index (PDI) of 0.2 [21]. A small ratio of about 29.6% of TiO₂ particles was 272.8 nm in size with the same PDI.

The particle size distribution of the fluorinated titanium nanoparticles determined by the DLS technique revealed that the particle size distribution of fluorinated titanium nanoparticles ranges approximately from 120 nm to 200 nm with an average particle size (hydrodynamic diameter) of 161.9 nm and PDI of 0.7. The size distribution of fluorinated nanoparticles is more uniform with a narrow distribution range (Figure 5. (B)). FTPs have a larger average hydrodynamic size than virgin TiO₂ because the TiO₂ surface is acquired via the chemical modification of FAS [20].

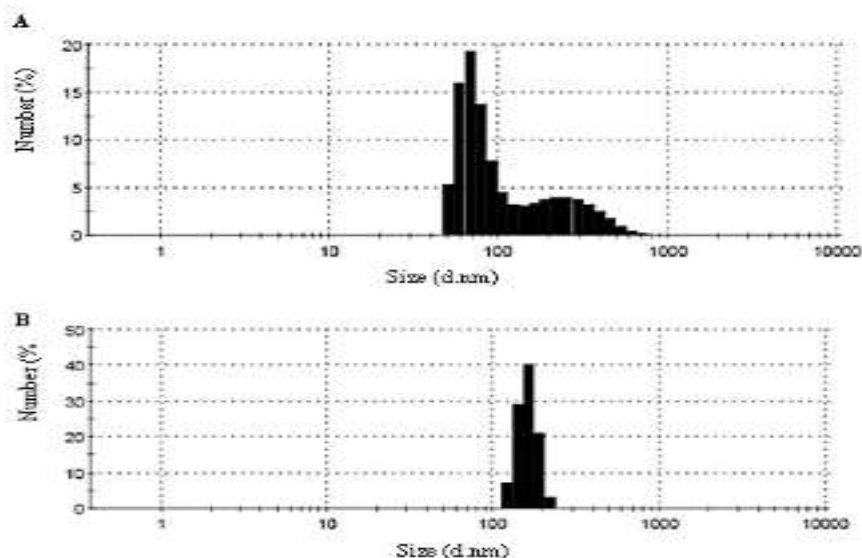


Fig. 5: Particle size distribution of the hydrodynamic diameter (d) of (A) the virgin and (B) fluorinated TiO₂ particles obtained by DLS number-weighted.

5.3 Membrane morphology

The SEM images of surface morphology at 4000x magnification for P₁, P₂ and P₃ are combined in Figure 6. Also, figure 6 (d) shows an enlarged picture at 11000x for P₃ at 11000x to detect its micro/nano structure. It was indicated that the porosity of membranes was enhanced after adding fluorinated TiO₂ nanoparticles, which accelerated the phase inversion process occurred in membranes preparation [22]. The P₁ and P₂ morphologies of the membranes had no significant changes before and after silane modification, as shown in Figure.6 (a) and (b). Nevertheless, some small differences were observed in high magnifications. We could see that plenty of pores in PVDF/FTP membranes surface have a nano size diameter (300-500nm). The pore sizes of the membranes decreased because of the filling of the membrane pores by entrapping inorganic FTPs in the polymeric matrix. This results in improved membrane porosity and an increase in the number of small pores with micro and nanostructures. The cross-linked structure of the PVDF entangled the FTPs through attractive electrostatic forces which lead to form micro/nano structures. This structure is due to the positive contribution of the low surface tension fluorocarbon compound in FTPs particles [23].

5.4 Surface roughness

Surface roughness, in combination with low surface energy, has an important role in improving the anti-wetting performance of a membrane. The topographical pictures produced by the AFM were used to further examine the surface roughness of the prepared membranes. Three-dimensional photo in Figure 7 demonstrates that the addition of FTPs and the surface modification silane solution changed the surface roughness. The P₃ membrane recorded the highest surface roughness. This nano-structure with multi-scale roughness was conducive to an excellent super-hydrophobic effect. Interestingly, PVDF/FTP membrane (P₃) exhibited hydrophobic characteristics as shown in Figure 7. It should be mentioned that increasing surface roughness using FTPs could result in more hydrophobic surface [24, 25].

The highest point of the membrane surface is indicated by the brightest area in the AFM images at a scan size of 50 nm, while the darkest areas show valleys or membrane pores. This reveals that the inclusion of FTP nanoparticles in the casting dope has an impact on the surface morphologies of membranes. It visually seems that the surface porosities of P₃ membranes prepared by adding 3 wt.% of FTPs are high compared to other membranes as shown in Figure 7 [23].

membrane with silane solution showed relatively higher hydrophobicity (117.8) with water. Enhancements in the CAs with water (121.7) was observed for the membrane P₃ which had a FTPs in their structure as illustrated in figure 8. The membrane prepared with FTPs possessed the highest hydrophobic surface, which enhanced their phenol repellent and superhydrophobic property [26].

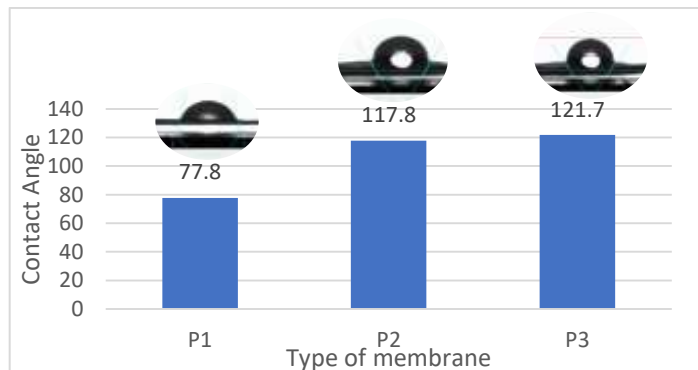


Fig. 8: Water droplet contact angle on the prepared membrane.

5.6 Membrane porosity

Water vapour flux in MD membranes is significantly related to membrane porosity and thickness, as commonly established in the literature. Table 3 shows the porosity of all prepared membranes. By increasing membrane porosity, the amount of vapour transferred through the membrane increases [28]. The porosity of all membranes used is quite high, and ranges between 66% and 80%. The porosity reached 80% when the P₃ membrane used, which affect membrane morphology.

Table 2: Porosity all membrane prepared

Membranes	P1	P2	P3
Porosity %	66	77	80

5.7 Mechanical properties

Table 2 shows the results of stress, strain and young’s modulus for the prepared membranes P₁, P₂ and P₃. The results were taken as average value of three recorded results for the same membrane. P₃ membrane gave the highest displacement (3.66 mm) as a result it posed the highest strain percentage. Based on Table 2, P₃ membrane shows an increase in strength value to 102.65 MPa when FTPs were used in the dope solution However, the strain value is slightly increased. As a result, the mechanical strength of the membrane is increased by the addition of FTPs to PVDF dope solution, which also affects membrane life [27].

Table 3: Mechanical properties of membranes of flat sheet membranes.

Membrane	Displacement, mm	Tensile stress, MPa	Young’s modulus (MPa)	Tensile strain, %
P ₁	2.25	0.99	100.18	7.51
P ₂	2.83	0.88	96.19	9.44
P ₃	3.66	0.9	102.65	12.19

6 Membrane performance in VMD unit

6.1 Effect of feeding temperature

The prepared membrane samples P₁, P₂ and P₃ were tested using VMD unit at the different temperature of phenol feed solution (40, 60, 70 and 80°C). The permeation flux and phenol rejection were calculated for all membranes. table 4 represent the flux and concentrations of each feed and permeate. The best rejection results were observed when using P₃ membrane which impregnated with fluorinated titanium dioxide. These results represent good agreement with the previous discussion for the prepared membrane characterization.

Table 4: Performance for different membrane in MD unit.

	Conditions		Flux (l/m ² .h)	SR%
	Feed Temp (°c)	Time of immersing in silane (min)		
P ₁	40	0	8	72
P ₁	60	0	8.2	69
P ₁	70	0	8.5	67
P ₁	80	0	9	65
P ₂	40	10	8.5	78
P ₂	60	10	8.72	79
P ₂	60	15	8.9	79.5
P ₂	60	30	8.8	81
P ₂	70	30	8.93	81.5
P ₃	40	0	9.5	89.5
P ₃	60	0	9.8	90
P ₃	70	0	10.2	90.2
P ₃	80	0	10.5	90.5

6.2 Effect of PH adjustment for the phenol feed solution

Phenol in aqueous solutions exists in two forms: volatile phenol molecules (C₆H₅OH) and less volatile phenolate ions (C₆H₅O). It is reasonable to infer that; addition of strong base (NaOH) to the reaction medium enhanced transformation of more volatile phenol molecules to less volatile phenolate ions, this causes that phenol remains in feed as phenolate ions that can be recovered easily [15, 29].

According to literature [4, 15, 29], the maximum level of phenolate ions were obtained at pH ranging from 10 to 12, so in this work, for effective separation of phenolate ions the experiment was conducted at PH 12. The obtained results of flux and phenols removal of feed solution at PH 12 and temperature 30°C were 6.19 lit/m².h and 90.2%, respectively. With increasing in feeding temperature to 80°C, the flux enhanced to 11.3 lit/m².hr and phenol was removed by 92.2%.

7 Conclusions

MD was successfully used for concentration of phenolic solution. An experimental study of VMD process using prepared membranes to treat phenolic wastewater was carried out. Effects of feed temperature and feed pH on phenol separation were also studied. Compared to a membrane without modification, a greater phenolic rejection was attained utilizing PVDF/FTPs membrane. The permeate flux was influenced by membrane porosity and hydrophobicity. Future studies should focus on enhancing membrane characterization to address the limited permeate flux.

References

- [1] Ozdemir, S., M. Buonomenna, and E. Drioli, Catalytic polymeric membranes: Preparation and application. Applied Catalysis A: General, 2006. 307(2): p. 167-183.

- [2] Mixa, A. and C. Staudt, Membrane-Based Separation of Phenol/Water Mixtures Using Ionically and Covalently Cross-Linked Ethylene-Methacrylic Acid Copolymers. *International Journal of Chemical Engineering*, 2008. 2008: p. 1-12.
- [3] Okiel, K., et al., Performance assessment of synthesized CNT/polypropylene composite membrane distillation for oil field produced water desalination. *Desalination and Water Treatment*, 2015. 57(24): p. 10995-11007.
- [4] Mohamad Said, K.A., et al., A review of technologies for the phenolic compounds recovery and phenol removal from wastewater. *Process Safety and Environmental Protection*, 2021. 151: p. 257-289.
- [5] Bolto, B., et al., A Review on Current Development of Membranes for Oil Removal from Wastewaters. *Membranes (Basel)*, 2020. 10(4).
- [6] El-Naas, M.H., S. Al-Zuhair, and M.A. Alhajja, Removal of phenol from petroleum refinery wastewater through adsorption on date-pit activated carbon. *Chemical Engineering Journal*, 2010. 162(3): p. 997-1005.
- [7] Mohammadi, S., et al., Phenol removal from industrial wastewaters: a short review. *Desalination and Water Treatment*, 2014. 53(8): p. 2215-2234.
- [8] Villegas, L.G.C., et al., A Short Review of Techniques for Phenol Removal from Wastewater. *Current Pollution Reports*, 2016. 2(3): p. 157-167.
- [9] Das, R., *Carbon Nanotube in Water Treatment*. 2017: p. 23-54.
- [10] Saputera, W.H., et al., Technology Advances in Phenol Removals: Current Progress and Future Perspectives. *Catalysts*, 2021. 11(8): p. 998.
- [11] Hamzah, N. and C.P. Leo, Fouling prevention in the membrane distillation of phenolic-rich solution using superhydrophobic PVDF membrane incorporated with TiO₂ nanoparticles. *Separation and Purification Technology*, 2016. 167: p. 79-87.
- [12] Das, R., et al., Carbon nanotube membranes for water purification: A bright future in water desalination. *Desalination*, 2014. 336: p. 97-109.
- [13] Drioli, E., et al., Novel PVDF hollow fiber membranes for vacuum and direct contact membrane distillation applications. *Separation and Purification Technology*, 2013. 115: p. 27-38.
- [14] Khayet, M., C. García-Payo, and T. Matsuura, Superhydrophobic nanofibers electrospun by surface segregating fluorinated amphiphilic additive for membrane distillation. *Journal of Membrane Science*, 2019. 588: p. 117215.
- [15] Fan, H., et al., Preparation and characterization of hydrophobic PVDF membranes by vapor-induced phase separation and application in vacuum membrane distillation. *Journal of Polymer Research*, 2013. 20(6).
- [16] Zhao, L., et al., Activated carbon enhanced hydrophobic/hydrophilic dual-layer nanofiber composite membranes for high-performance direct contact membrane distillation. *Desalination*, 2018. 446: p. 59-69.
- [17] Alhathal Alanezi, A., et al., Performance Investigation of O-Ring Vacuum Membrane Distillation Module for Water Desalination. *Journal of Chemistry*, 2016. 2016: p. 1-11.
- [18] E.M. Hamad, S. Al-Gharabli, J. Kujaw, 2022, Tunable hydrophobicity and roughness on PVDF surface by grafting to mode – Approach to enhance membrane performance in membrane distillation process, *Separation and Purification Technology*, vol.291, 120935.
- [19] E.J. Lee, A.K. An, P. Hadi, S. Lee, Y.C. Woo, H.K. Shon, 2017, Advanced multi-nozzle electrospun functionalized titanium dioxide/ polyvinylidene fluoride-co-hexafluoropropylene (TiO₂ /PVDF-HFP) composite membranes for direct contact membrane distillation, *Journal of Membrane Science*, vol. 524, pp.712–72.
- [20] F. Tibi , S.-J. Park, J. Kim, 2021, Improvement of Membrane Distillation Using PVDF Membrane Incorporated with TiO₂ Modified by Silane and Optimization of Fabricating Conditions, *Membranes* , vol.11, 95.
- [21] F. Edwie, M.M. Teoh, T.S. Chung, 2012, Effects of additives on dual-layer hydrophobic–hydrophilic PVDF hollow fiber membranes for membrane distillation and continuous performance, *Chemical Engineering Science*, vol. 68, pp. 567–57.
- [22] Guangyong Zeng Yi He Zongxue Yu Yingqing Zhan Lan Ma Lei Zhang, Preparation and characterization of a novel PVDF ultrafiltration membrane by blending with TiO₂-HNTs nanocomposites, *Applied Surface Science* <http://dx.doi.org/10.1016/j.apsusc.2016.02.211>
- [23] S. Bonyadi, T.S. Chung, W.B. Krantz, 2007, Investigation of corrugation phenomenon in the inner contour of hollow fibers during the non-solvent induced phase separation process, *Journal of Membrane Science*. vol. 299, pp. 20-210.

- [24] Razmjou, E. Arifin, G. Dong, J. Mansouri, V. Chen, 2012 Superhydrophobic modification of TiO₂ nanocomposite PVDF membranes for applications in membrane distillation, *Journal of Membrane Science*, vol. 415–416, pp. 850–8
- [25] L.G. Fernández, 2017, Design, preparation and characterization of hollow fiber membranes for desalination by membrane distillation, *Doctoral Thesis*, Madrid.
- [26] W. Zhang, Y. Li, J. Liu, B. Li, S. Wang, 2017, Fabrication of hierarchical poly (vinylidene fluoride) micro/nano-composite membrane with anti-fouling property for membrane distillation, *Journal of Membrane Science*, vol. 535, pp. 258–26.
- [27] R. Das, Md. Equb Ali, S.B. Abd Hamid, S. Ramakrishna, Z.Z. Chowdhury, 2014, Carbon nanotube membranes for water purification: A bright future in water desalination. *Desalination*, vol. 336, pp. 97-109.
- [28] N. Hamzah and C.P. Leo, 2016, Fouling prevention in the membrane distillation of phenolic- rich solution using superhydrophobic PVDF membrane incorporated with TiO₂ nanoparticles, *Separation and Purification Technology*, vol. 167, pp. 79–87, <https://doi.org/10.1016/j.seppur.2016.05.005>.
- [29] Toraj Mohammadi, Pezhman Kazemi, Taguchi optimization approach for phenolic wastewater treatment by vacuum membrane distillation, *Desalination and Water Treatment*.